

## Coordination Bond Formation at Charge-Transfer Phase Transition in $(\text{BDTA})_2[\text{Co}(\text{mnt})_2]$

Yoshikatsu Umezono,<sup>†</sup> Wataru Fujita,<sup>‡</sup> and Kunio Awaga<sup>\*†</sup>

Department of Chemistry, Graduate School of Science, Nagoya University, Chikusa-ku, Nagoya 464-8602, Japan, and Research Center of Materials Science, Nagoya University, Chikusa-ku, Nagoya 464-8602, Japan

Received October 29, 2005; E-mail: awaga@mbox.chem.nagoya-u.ac.jp

Electronic properties of molecular crystals have been studied extensively,<sup>1</sup> and some unique phase transitions have been found to result from an electronic instability or bistability through a strong electron–lattice interaction.<sup>2</sup> A typical example is the charge-transfer (CT) phase transition associated with an intermolecular electron transfer during the structural change. A donor–acceptor-type organic CT complex, TTF–chloranil, exhibits a neutral–ionic phase transition, at which the degree of charge transfer changes from 0.3 to 0.7 with various critical phenomena including quantum behavior.<sup>3</sup> Recently, CT phase transitions have been observed in several transition metal complexes.<sup>4</sup> In the present communication, we report a CT phase transition in the 2:1 complex of a thiazyl radical, BDTA (1,3,2-benzodithiazolyl),<sup>5</sup> and a cobalt–dithiolene complex,  $[\text{Co}(\text{mnt})_2]$  ( $\text{mnt}^{2-}$  = maleonitriledithiolate) (see the inset of Figure 1), which is accompanied by characteristic changes in molecular structure, intermolecular packing, and magnetic susceptibility.

$(\text{BDTA})_2[\text{Co}(\text{mnt})_2]$  was prepared by the reaction of  $\text{BDTA}\cdot\text{Cl}^{5a}$  and  $[\text{N}(\text{C}_4\text{H}_9)_4]_2[\text{Co}(\text{mnt})_2]^{6}$  in a 1:1 solvent mixture of dry methanol and ethanol. After filtration, the filtrate was set at  $-23\text{ }^\circ\text{C}$  for one night, during which rather air-sensitive, block-shape crystals of  $(\text{BDTA})_2[\text{Co}(\text{mnt})_2]$  were grown.

The magnetic properties of  $(\text{BDTA})_2[\text{Co}(\text{mnt})_2]$  were investigated in the temperature range of 2–300 K under 1 T on a Quantum-Design MPMS XL SQUID susceptometer. The experimental raw data were corrected for diamagnetism, and the paramagnetic susceptibilities,  $\chi_p$ , were obtained. The results are depicted in Figure 1, where the values of  $\chi_p T$  are plotted against temperature  $T$ . In the temperature range of 200–300 K, the  $\chi_p T$  value ( $0.61\text{ emu K mol}^{-1}$ ) depended little on temperature, obeying the Curie law. Upon cooling, however,  $\chi_p T$  rapidly decreased down to  $0.49\text{ emu K mol}^{-1}$  at 180 K, followed by a Curie–Weiss behavior with a Weiss constant of  $\theta = -4.7\text{ K}$ . Figure 1 also shows the  $\chi_p T$  values upon heating, revealing a hysteresis loop of 20 K at the transition. This indicates that the anomaly at 190 K was caused by a first-order phase transition.

Since the magnetic data indicated a structural phase transition at 190 K, we carried out single-crystal X-ray analyses at 253 and 100 K.<sup>7</sup> Figure 2a shows a view of the unit cell at 253 K, in which one-half of the  $(\text{BDTA})_2[\text{Co}(\text{mnt})_2]$  unit is crystallographically independent. BDTA occurs as a head-to-head dimer formed by short  $\text{S}\cdots\text{N}$  and  $\text{N}\cdots\text{N}$  contacts. This dimer unit and the planar  $[\text{Co}(\text{mnt})_2]$  form an alternating stacking column along the  $b$  axis, indicating a large  $\pi$  overlap between them. In this column, the axial positions of the cobalt ion are occupied by the sulfurs on separate BDTA molecules at a distance of  $3.1672(9)\text{ \AA}$ , though this value is nearly the same as the interplanar distance. This is in agreement

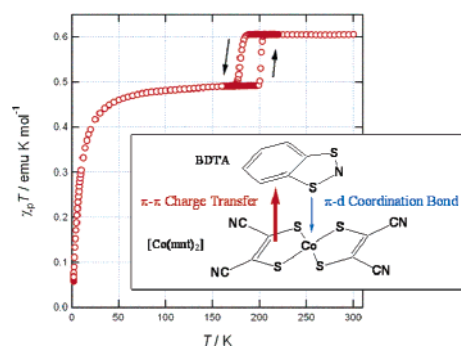


**Figure 1.** Temperature dependence of  $\chi_p T$  for  $(\text{BDTA})_2[\text{Co}(\text{mnt})_2]$ . The inset shows a possible mechanism of coordination bond formation at the phase transition of 190 K.

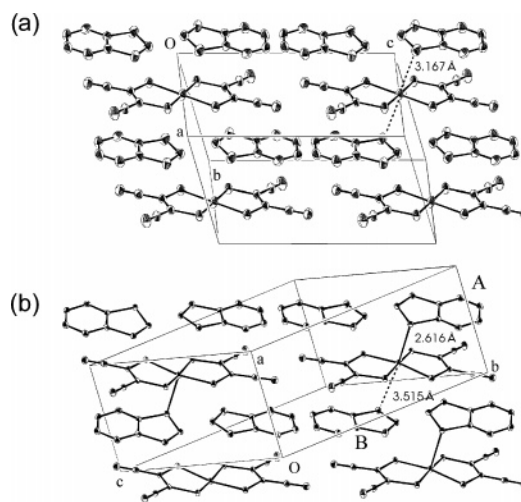


**Figure 2.** Crystal structures of  $(\text{BDTA})_2[\text{Co}(\text{mnt})_2]$  at 253 K (a) and 100 K (b).

with the fact that it is not likely for cationic species to be ligands of metal ions due to their positive charge.

It is known that the S–N bond length,  $l_{\text{SN}}$ , of BDTA is a good indicator of the charge,  $\rho_{\text{BDTA}}$ , on it. The removal of the unpaired electron in the SOMO (singly occupied molecular orbital) of BDTA shortens the S–N bond lengths because the SOMO has an antibonding character on the S–N bonds. Figure 3 shows the relation between  $l_{\text{SN}}$  and  $\rho_{\text{BDTA}}$ ;  $l_{\text{SN}}$  is  $1.646(2)\text{ \AA}$  on average for the neutral BDTA and  $1.598(2)\text{ \AA}$  for  $\text{BDTA}^+\cdot\text{Cl}^-\cdot\text{SO}_2$ .<sup>5b</sup> This figure also includes the plot for the  $\text{BDTA}^+\cdot\text{TCNQ}$ , which is in a mixed valence state;  $l_{\text{SN}}$  is  $1.619(4)\text{ \AA}$ ,<sup>8</sup> and  $\rho_{\text{BDTA}}$  can be estimated to be 0.63 from the CN stretching frequency of TCNQ ( $2196\text{ cm}^{-1}$ ).<sup>9</sup> This figure indicates an empirical linear relation between  $l_{\text{SN}}$  and  $\rho_{\text{BDTA}}$ . The two S–N bond lengths in  $(\text{BDTA})_2[\text{Co}(\text{mnt})_2]$  are  $1.598(2)$  and  $1.608(2)\text{ \AA}$  at 253 K, so that, by fitting the average

<sup>†</sup> Department of Chemistry.

<sup>‡</sup> Research Center of Materials Science.

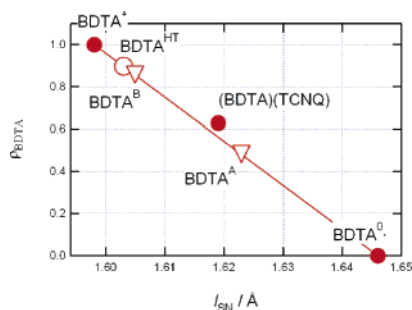


**Figure 3.** Correlation between the charge and the S–N bond length in BDTA compounds.

value to the relation,  $\rho_{\text{BDTA}}$  is estimated to be 0.9 (open circle in Figure 3). This corresponds to the formula  $(\text{BDTA}^{0.9+})_2[\text{Co}(\text{mnt})_2]^{1.8-}$  for the high-temperature phase. Since  $\text{BDTA}^+$  and  $[\text{Co}(\text{mnt})_2]^{2-}$  are  $S = 0$  and  $1/2$  spin species, this formula unit possesses one unpaired electron.

Figure 2b shows the crystal structure at 100 K that includes two crystallographically independent BDTA molecules, A and B. The packing features resembled those observed at 253 K, but the structure included a crucial difference; there was a  $\text{Co}\cdots\text{S}$  axial coordination bond of 2.6163(18) Å between  $\text{BDTA}^{\text{A}}$  and  $[\text{Co}(\text{mnt})_2]$ , while the  $\text{Co}\cdots\text{S}$  distance was 3.5152(16) Å on the B side. Moreover,  $\text{BDTA}^{\text{A}}$  was significantly different in molecular structure; the average S–N bond length,  $l_{\text{SN}}$ , for  $\text{BDTA}^{\text{A}}$  (1.623(3) Å) is much longer than those for  $\text{BDTA}^{\text{B}}$  (1.605(3) Å) and BDTA in the high-temperature phase (1.603(2) Å). From the relation in Figure 3, the charges on the two BDTA molecules were estimated to be  $\rho_{\text{BDTA}^{\text{A}}} \approx 0.5$  and  $\rho_{\text{BDTA}^{\text{B}}} \approx 0.9$ , respectively. These values suggested a partial CT at the phase transition, namely,  $(\text{BDTA}^{0.9+})_2[\text{Co}(\text{mnt})_2]^{1.8-}$  (253 K)  $\rightarrow$   $(\text{BDTA}^{0.9+})(\text{BDTA}^{0.5+})[\text{Co}(\text{mnt})_2]^{1.4-}$  (100 K).

The structural analyses indicated a partial CT by ca. 0.4 for the phase transition at 190 K. This was further supported by the  $g$ -factors for the two phases, which were estimated from the Curie constants obtained by magnetic measurements to be  $g = 2.55 \pm 0.10$  and  $2.29 \pm 0.10$  for the high- and low-temperature phases, respectively. The error bars are mainly caused by the air sensitivity of the present compound. Since the  $g$ -factor is governed by the distribution of the unpaired electron in the  $(\text{BDTA})_2[\text{Co}(\text{mnt})_2]$  unit, it can be written as

$$g^2 = (2 - 2\bar{\rho}_{\text{BDTA}}) g_{\text{BDTA}}^2 + (2\bar{\rho}_{\text{BDTA}} - 1) g_{[\text{Co}(\text{mnt})_2]}^2 \quad (1)$$

where  $\bar{\rho}_{\text{BDTA}}$  is the average charge on BDTA, and  $g_{\text{BDTA}}$  (2.006) and  $g_{[\text{Co}(\text{mnt})_2]}$  (2.526 of  $[\text{N}(\text{C}_4\text{H}_9)_4]_2[\text{Co}(\text{mnt})_2]$ )<sup>8</sup> are the  $g$ -factors for the neutral  $S = 1/2$  BDTA radical and the  $S = 1/2$   $[\text{Co}(\text{mnt})_2]^{2-}$  dianion, respectively. Using the values of  $\bar{\rho}_{\text{BDTA}}$  indicated in the structural analyses, 0.9 and 0.7 for the high- and low-temperature phases, the two  $g$ -factors are calculated to be 2.43 and 2.23, respectively. These values are roughly in agreement with the corresponding values estimated from the Curie constants; the magnetic jump at the phase transition can be explained by the partial CT between BDTA and  $[\text{Co}(\text{mnt})_2]$ .

The structural and magnetic analyses revealed the CT phase transition,  $(\text{BDTA}^{0.9+})_2[\text{Co}(\text{mnt})_2]^{1.8-}$  (253 K)  $\leftrightarrow$   $(\text{BDTA}^{0.9+})(\text{BDTA}^{0.5+})[\text{Co}(\text{mnt})_2]^{1.4-}$  (100 K). This change in the degree of CT is smaller than those for the other CT transitions in the transition

metal complexes;<sup>3,4</sup> that such a small change should bring about the coordination bond formation is peculiar to the present transition. This can be qualitatively explained (the inset of Figure 1). The electron transfer from  $[\text{Co}(\text{mnt})_2]^{2-}$  to  $\text{BDTA}^+$  through the  $\pi$  overlap decreases the positive charge on  $\text{BDTA}^+$  and enhances the ability of BDTA to act as a ligand. Thus, BDTA forms a coordination bond, giving back the obtained electron partially to the vacant d orbitals of the cobalt ion in  $[\text{Co}(\text{mnt})_2]$ . This back-donation makes the degree of CT smaller as a result. Another possible reason is the stability of  $\text{BDTA}^+$  compared with the neutral BDTA radical having an unstable unpaired electron.

Cyclic thiazyl radicals are attracting much interest because of their unique solid-state properties, such as magnetic bistability,<sup>10</sup> and of effectiveness as building blocks of supramolecular electrical and/or magnetic materials.<sup>11</sup> So far the bistabilities of thiazyl radicals were caused by different intermolecular arrangements in the crystals, but the present bistability is due to switching between bonding and dissociation of the coordination bond, which is considered to reflect a competing duality of BDTA as cation and ligand.

**Acknowledgment.** The authors would like to thank Toshihiko Yokoyama and Tamotsu Inabe for helpful discussion, and Hirofumi Yoshikawa for assistance in crystallographic analysis. This work was supported by the Grant-in-Aid for Scientific Research from the Ministry of Education, Science, and Culture, Japan.

**Supporting Information Available:** Crystallographic data of  $(\text{BDTA})_2[\text{Co}(\text{mnt})_2]$  at 253 and 100 K. This material is available free of charge via Internet at <http://pubs.acs.org>.

## References

- (1) (a) Molecular Conductors. *Chem. Rev.* **2004**, *104*. (b) Miller, J. S. In *Magnetism: Molecules to Materials*; Drillon, M., Ed.; Wiley-VCH: Weinheim, Germany, 2001.
- (2) Sorai, M. *Bull. Chem. Soc. Jpn.* **2001**, *74*, 2223.
- (3) (a) Torrance, J. B.; Vazquez, J. E.; Mayerle, J. J.; Lee, V. Y. *Phys. Rev. Lett.* **1981**, *46*, 253. (b) Horiuchi, S.; Okimoto, Y.; Kumai, R.; Tokura, Y. *Science* **2003**, *299*, 229 and references therein.
- (4) (a) Kojima, N.; Aoki, W.; Itoi, M.; Ono, Y.; Seto, M.; Kobayashi, Y.; Maeda, Y.; *Solid State Commun.* **2001**, *120*, 165. (b) Mochida, T.; Takazawa, K.; Takahashi, M.; Takeda, M.; Nishio, Y.; Sato, M.; Kajita, K.; Mori, H.; Matsushita, M. M.; Sugawara, T. *J. Phys. Soc. Jpn.* **2005**, *74*, 2214. (c) Tokoro, H.; Ohkoshi, S.; Matsuda, T.; Hashimoto, K. *Inorg. Chem.* **2004**, *43*, 5231.
- (5) (a) Wolmershäuser, G.; Schnauber, M.; Wilhelm, T. *J. Chem. Soc., Chem. Commun.* **1984**, 573. (b) Awere, E. G.; Byeford, N.; Haddon, R. C.; Parsons, S.; Passmore, J.; Waszczak, J. V.; White, P. S. *Inorg. Chem.* **1990**, *29*, 4821. (c) Fujita, W.; Awaga, K.; Nakazawa, Y.; Saito, K.; Sorai, M. *Chem. Phys. Lett.* **2002**, *352*, 348.
- (6) Billing, E.; Williams, R.; Bernal, I.; Waters, J. H.; Gray, H. B. *Inorg. Chem.* **1964**, *3*, 663.
- (7) (a) Crystal data at 253 K:  $\text{C}_{20}\text{H}_8\text{CoN}_6\text{S}_8$ ,  $M = 647.73$ , triclinic, space group  $P\bar{1}$ ,  $a = 7.0174(17)$  Å,  $b = 7.2752(18)$  Å,  $c = 12.901(4)$  Å,  $\alpha = 78.989(9)^\circ$ ,  $\beta = 79.253(9)^\circ$ ,  $\gamma = 70.956(8)^\circ$ ,  $V = 605.6(3)$  Å<sup>3</sup>,  $Z = 1$ ,  $R = 0.0334$ ,  $wR = 0.0778$ . (b) Crystal data at 100 K: triclinic, space group  $P\bar{1}$ ,  $a = 7.212(4)$  Å,  $b = 13.392(8)$  Å,  $c = 14.121(9)$  Å,  $\alpha = 115.484(7)^\circ$ ,  $\beta = 101.650(7)^\circ$ ,  $\gamma = 90.923(6)^\circ$ ,  $V = 1197.5(12)$  Å<sup>3</sup>,  $Z = 2$ ,  $R = 0.0443$ ,  $wR = 0.0923$ .
- (8) Umezono, Y.; Fujita, W.; Awaga, K.; Cui, H. B.; Kobayashi, H. Unpublished work.
- (9) Chappel, J. S.; Bloch, A. N.; Bryden, W. A.; Maxfield, M.; Poehler, T. O.; Cowan, D. O. *J. Am. Chem. Soc.* **1981**, *103*, 2442.
- (10) (a) Fujita, W.; Awaga, K. *Science* **1999**, *286*, 261. (b) Fujita, W.; Awaga, K.; Matsuzaki, H.; Okamoto, H. *Phys. Rev. B* **2002**, *65*, 064434. (c) Brusso, J. L.; Clements, O. P.; Haddon, R. C.; Itkis, M. E.; Leitch, A. A.; Oakley, R. T.; Reed, R. W.; Richardson, J. F. *J. Am. Chem. Soc.* **2004**, *126*, 8256 and 14692.
- (11) (a) Rawson, J. M.; Palacio, F. *Struct. Bonding* **2001**, *100*, 93. (b) Bryan, C. D.; Cordes, A. W.; Fleming, R. M.; George, N. A.; Glarum, S. H.; Haddon, R. C.; Oakley, R. T.; Palstra, T. T.; Perel, A. S.; Schneemeyer, L. F.; Waszczak, J. V. *Nature* **1993**, *365*, 821.

JA057207I